Biological H_2(g) Production and Modelling with Computational Fluid Dynamics (CFD)

RUKİYE ÖZTEKİN*, DELİA TERESA SPONZA
Department of Environmental Engineering,
Dokuz Eylül University,
Tınaztepe Campus, 35160 Buca/Izmir,
TURKEY

**Corresponding Author*

Abstract: - In this study, bio-hydrogen gas [bio-H_2(g)] production and modeling with a three-phase computational fluid dynamics (CFD) model, heat and mass transfer of bio-hydrogen production, reaction kinetics, and fluid dynamics; It was investigated by dark fermentation process in an anaerobic continuous plug flow reactor (ACPFR). The three-phase CFD model was used to determine the bio-H_2(g) production in an ACPFR. The effect of different operating parameters, increasing hydrolic retention times (HRTs) (1, 2, 4, 8, and 12 days), different pH values (4.0, 5.0, 6.0, 7.0, and 8.0), and increasing feed rate as organic loading rates (OLRs) (0.5, 1.0, 2.0, 4.0, 8.0 and 10.0 g COD/l.d) on the bio-H_2(g) production rates were operated in municipal sludge wastes (MSW) with *Thermoanaerobacterium thermosaccharolyticum* SP-H2 methane bacteria during dark fermentation for bio-H_2(g) production. The effect of HRT, pH, and feed rate on the bio-H_2(g) efficiencies and H_2(g) production rates were examined in the simulation stage. Production of volatile fatty acids (VFAs) namely, acetic acids, butyric acids, and propionic acids were important points influencing the bio-H_2(g) production yields. The artificial neural network (ANN) model substrate inhibition on bio-H_2(g) production to the methane (CH_4) bacteria was also investigated. The reaction kinetics model used *Thermotoga neapolitana* microorganisms with the Andrews model of substrate inhibition. Furthermore, the ANN model was well-fitted to the experimental data to simulate the bio-H_2(g) production from chemical oxygen demand (COD).

Key-Words: - Acetic acids; Anaerobic continuous plug flow reactor (ACPFR); Artificial neutral network (ANN) model; Biological hydrogen gas [Bio-H(g)] production; Butyric acids; Computational fluid dynamics (CFD) model; Propionic acids; *Thermoanaerobacterium thermosaccharolyticum* SP-H2; *Thermotoga neapolitana*, Volatile fatty acids (VFAs).

Received: August 18, 2022. Revised: October 15, 2023. Accepted: November 17, 2023. Published: December 12, 2023.

1 Introduction

The technologies of energy production based on burning fossil fuels constitute the world's main energy production source and cause pollution and degradation of the natural environment, [1], [2]. Fossil fuels and non-renewable energy; It causes environmental damage and climate change by causing destruction in soil, water, and air. The partial and complete combustion of fossil fuels emits greenhouse pollutants like CO_x, NO_x, SO_x, C_xH_y, ash, and other organic compounds in the environment, [3]. For energy production based on renewable resources; New clean technologies need to be developed, [4], [5]. The development of these technologies is supported by social pressure, carbon neutrality requirements, the political environment, and appropriate legal regulations. Because it reduces carbon dioxide [CO_2(g)] and methane [CH_4(g)] emissions into the air and has the potential to improve the quality of life of future generations; It fits the main theme of the decarboxylation approach. An increase in new renewable energy expenditures, technologies that include the energy use of biomass to bio-H_2(g) may provide a solution to these challenges, [6].

H_2(g) is nontoxic, colorless, odorless, [7], tasteless, and the third most abundant element on Earth, [8]. H_2(g) as an environmentally friendly gas is an energy carrier that could play a significant role in the reduction of greenhouse gases, [9], [10]. Due to water (H_2O) production during the combustion process, H_2(g) is considered a clean fuel. H_2(g) is regarded as an ideal energy with a high energy yield of 122 kJ/g, which is 2.75 folds greater than that of hydrocarbon fuels, [11]. For this reason, H_2(g) is

one of the cleanest and most promising energy sources.

In comparison with conventional anaerobic process [fermentative CH_4(g) production], due to some inconsistency and drawbacks, the H_2(g) production processes by dark fermentation are less well developed than the CH_4(g) production. During anaerobic digestion of organic wastes, such as solid waste and wastewater, CH_4(g) is produced and its production processes have been well established commercially. H_2(g) is a more valuable energy carrier and chemical feedstock compared with CH_4(g), [12], [13]. Therefore, dark fermentation can treat agro-industrial effluents and also valorized them through energy production, [12]. However, a bottleneck for the widespread utilization of these processes is the relatively low hydrogen production rates (HPR), and thus several strategies to enhance it have been proposed, [14]. One of them is the use of feedback control, which is the case explored in this communication. Different ways of H_2(g) production methods are summarized at Figure 1 (Appendix).

Bio-H_2(g) is a feasible, promising, and clean alternative fuel with no CO_2(g) emissions and high energy content per unit weight (141.9 J/kg); Additionally, only H_2O is produced as a result of H_2(g) combustion, [15]. Using the dark fermentation process, organic wastes can be decomposed into bio-H_2(g), CO_2(g), and VFAs, and converted into metabolites, which can be utilized in other fermentation processes based on the carboxylate platform, [16]. Considering the conventional treatment costs and the energy and chemical needs in the processes used, by reducing the carbon footprint; Dark fermentation, which produces clean and renewable H_2(g) from wastewater, is an alternative to reduce fossil fuel consumption, [17]. It compared different methods applied for H_2(g) production, such as photo-fermentation, dark fermentation, electrolysis, electrodialysis and photocatalysis, which include environmental, economic, energy and energetic impacts, [18]. According to Bio-H_2(g) production methods, the most economical and efficient process occurs in dark fermentation (Figure 2, Appendix).

Biological H_2(g) production offers many advantages, such as clean gas, simple technology, and cheap high-intensity energy (122 kJ/g). Additionally, its use does not produce any greenhouse gases and has some significant economic and environmental advantages. Biofuels are considered solid, liquid, and gaseous fuels produced predominantly using biomass. Various fuels such as ethanol, methanol, H_2(g), and CH_4(g) can be obtained from biomass, [19]. Plant biomass, from which biofuels are produced, accumulates solar energy. First-generation biofuels are produced using traditional methods such as fermentation or esterification, which do not require large amounts of energy. In the case of traditionally so-called first-generation biofuels, production is based on edible plants such as sugar beet root, corn, sugarcane, cereals, potatoes (starch), or vegetable oils (such as rapeseed, palm, or jatropha). In contrast, bioethanol is produced through alcoholic fermentation, while biodiesel is produced through the esterification of vegetable oils. Bio-H_2(g) production can be carried out in batch, fed-batch, and continuous modes. Reactor types for bio-H_2(g) production can be grouped as open and closed systems. Closed fermentation systems can be tubular reactors, bubble columns, or airlift systems. A bioreactor used in H_2(g) production significantly affects the efficiency and effectiveness of H_2(g) production.

Biological methods allow us to cost-effectively produce bio-H_2(g) via dark fermentation; Additionally, the photo-fermentation process can also be applied to produce bio-H_2(g) from various sources, [20], [21]. However, production efficiency largely depends on temperature, pH, and light intensity. Another method worth mentioning is the combined photo and dark fermentation method for bio-H_2(g) production, which can increase the production efficiency by 20% to 189%, [22]. Two-stage hybrid processes were applied to produce bio-H_2(g) from diluted solid waste, [23]. Typically, bio-H_2(g) production relies on a continuously stirred tank reactor; Tube anaerobic packed bed reactor can be considered a promising technology for bio-H_2(g) production because a high organic loading rate can be achieved by using recirculation and a large surface area to ensure better microorganism contact, [23].

The last few years have seen an increase in the use of more advanced techniques such as computational fluid dynamics (CFD) for the design and optimization of wastewater treatment systems. [24], [25], [26]. Bio-H_2(g) production CFD simulation tool is used to simulate all kinds of complex problems arising from the variability of parameters of biological models. CFD methods enable the determination of variables such as volume fraction, shear strain rate, or turbulent kinetic energy. They also facilitate the reliable prediction of the relevant hydrodynamic variables, the computational times, and fluid dynamics coupling, as well as mass transfer and kinetic variables. Additionally, the influence of inner geometry and mass phase transfer can be used in numerical simulations, [27]. Fluid particles pass

through the reactor with little or no longitudinal mixing and exit from the reactor in the same sequence in which they entered. Their identity remains in the reactor for a time equal to the theoretical detention time. This type of flow is approximated in long open tanks with a high length/width ratio where longitudinal dispersion is minimal or absent, [28]. Operational factors to be considered in selecting the type of reactor to be used in the treatment process include the nature of the wastewater to be treated, the nature of the reaction (homogeneous/heterogeneous), the reaction kinetics that governs the treatment process, process performance requirements, and local environmental conditions.

The integration of physical and biological processes still poses great challenges. Although it is necessary to develop and apply new methods to improve reactor hydrodynamics, heat, and mass transfer, [29], there are very few publications on modeling in packed bed bio-H_2(g) production, [30], [31]. CFD methods can be used to optimize the reactor configuration and therefore improve the performance of a bio-H_2(g) production reactor. CFD software is able to predict the hydrodynamics of fluid flow, heat and mass transfer, chemical reactions in a reactor, and other related events by solving a series of partial differential equations. Processes that describe mass, momentum, energy, and species balances are advanced methods that are widely and successfully used, [32], [33]. CFD is an effective tool for hydrodynamic-biokinetic analysis of anaerobic digestion of partial differential equations, [34]. It is complex because it requires a complex biological kinetic process using the user-defined function (UDF) written in C. It also allows optimizing performance costs without increasing the cost of prototyping, [35]. To see the flow pattern of the liquid, CFD can be used, which focuses on predicting hydrodynamic patterns through porous media. Flow dispersity patterns through a packed bed reactor resulted in arranged spherical particles using the discrete element method (DEM) coupling with a biokinetics model, which is an efficient method to predict bio-H_2(g) concentration in a continuous tube reactor, [36]. Parameters such as HRT, H_2(g) production rate, substrate conversion, pressure drop, and flow dispersity can be calculated by CFD to see the flow pattern of liquid through porous media, [37].

The artificial neural network (ANN) model is used to examine relationships in complex nonlinear data due to the data classification and learning ability of the ANN model; It is a good tool that is widely used and works according to human nervous systems and brain, [38], [39], [40], [41]. In the last decade, ANN models have been used in environmental engineering fields such as biological treatment of wastewater, membrane filtration, pollution adsorption, and electrodialysis of salt water, [38], [39], [40], [41].

Until now, there are few parameters for online monitoring in bioreactors, the most frequent are temperature, pH, oxidation-reduction potential (ORP), dissolved oxygen (DO), and dissolved CO_2. A useful approach is the use of mathematical models with these online determinations for the estimation of the fermentative products. For this purpose, the ANN has been successfully used, since they are based on the connectivity of biological neurons that have an incredible capability for emulation, analysis, prediction, association, and adaptation, [12], [42]. For instance, pH, temperature, and NaCl concentration were used to estimate maximum specific growth rate and bacteriocin production in *Streptococcus macedonicus* ACA-DC 198 cultures using feedforward ANNs, [43]. By applying a recurrent neural network, DO, feeding rate, and liquid volume were used to determine biomass concentration in *Saccharomyces cerevisiae* cultures, [42]. ORP, and backpropagation neural network were used to predict ethanol and biomass production in non-axenic cultures, [44].

Biomass gasification, as an attractive technology for the conversion of various types of biowastes to energy, is known to be a sustainable procedure to produce H_2(g), [45], [46]. The gasification of biowastes has been investigated in several research works from the view point of performance analysis, [47], [48], [49], [50], [51], [52], [53], [54], [55], [56], [57]. Nevertheless, just a few works on performance analysis of linked gasification–H_2(g) production have been reported, [58], [59], [60]. In order to have a comprehensive analysis of a H_2(g) production system via water–gas shift reactors, different modeling approaches based on thermodynamic equilibrium, kinetics, CFD, and ANNs can be developed. The models derived by equilibrium approaches are independent of the gasifier structure, so can be applied for ideal systems and typical thermodynamic characteristics. However, for a widely complex process, accurate kinetic parameters are needed that are used in kinetic modeling. In calculations relying on CFD, a series of equations of energy, momentum, mass, and species through a specific area of the gasifier are solved simultaneously and can then predict the distribution of temperature and concentration. The methods based on ANN require a huge amount of

data and then use a set of mathematical regressions for correlations among input and output data, [55], [61], [62], [63], [64], [65], [66]. This method has gained importance recently because it can estimate nonlinear functions without the need for a mathematical explanation of events in the system. However, when critical interactions of complex nonlinearities such as biomass conversion are included in a data set, ANN models are attractive for outcome prediction, [67], [68], [69], [70]. Therefore, very little work has been reported on modeling biomass gasification using the ANN model, and nothing in the field of downdraft gasifiers coupled with water-gas shift reactors for bio-H_2(g) production.

In this study, a new design project ACPFR model to analyze the heat and mass transfer, reaction kinetics, and fluid dynamics of bio-H_2(g) production through fermentation and full transient three-phase CFD modeling of bio-H_2(g) production was investigated. Different operating parameters, increasing HRTs (1, 2, 4, 8 and 12 days), different pH values (4.0, 5.0, 6.0, 7.0 and 8.0) and feed rate (0 .5, 1.0, 2.0, 4.0, 8.0) and 10.0 g COD/l.d) on bio-H_2(g) production rates, bio-H_2(g) yields and H_2(g) for its production, it was run in MSW with Thermoanaerobacterium thermosaccharolyticum SP-H2 methane bacteria during anaerobic dark fermentation in an ACPFR. Rates in the simulation phase; The production of VFAs, namely acetic, butyric, and propionic acids, are important points affecting bio-H_2(g) production efficiency. Furthermore, the aim of this study is to develop an ANN to predict H_2(g) production in genetically modified Thermoanaerobacterium thermosaccharolyticum SP-H2 fermentations based on online measurements of ORP, pH, and dissolved CO_2, respectively.

2 Materials and Methods

2.1 Microorganisms

The hydrogen-producing bacterium SP-H2 was isolated from a thermophilic acidogenic reactor inoculated with municipal sewage sludge and processed a carbohydrate-rich simulated food waste. Based on the 16S rRNA gene sequence, the bacterium was identified as *Thermoanaerobacterium thermosaccharolyticum* SP-H2. The maximum growth rate was observed at 55–60°C and at optimum pH=7.5.

2.1.1 Inoculum, Substrates, Mineral Medium

The effluent from the thermophilic acidogenic reactor, inoculated with municipal sewage sludge and treating high-strength simulated wastewater, [71], was used to isolate a new bacterial strain known as Thermoanaerobacterium thermosaccharolyticum SP-H2.

Pfennig`s medium, [72], containing the following: 330 mg/l NH_4Cl, 500 mg/l $MgCl_2.6H_2O$, 168 mg/l $CaCl_2$, 330 mg/l KCl, 330 mg/l KH_2PO_4 was used to isolate for Thermoanaerobacterium thermosaccharolyticum SP-H2 bacteria. The medium was supplemented with 500 mg/l yeast extract, 2500 mg/l $NaHCO_3$ as well as with a trace element solution, [73], and a vitamin solution, [74]. 0.5 g/l sodium sulfide and 0.5 g/l cysteine were used as reducing agents. The final pH was 6.8–7.0.

2 ml of effluent was inoculated into an 18 ml medium containing 5 g/l potato starch as the carbon source in a 60 ml serum bottle and cultured in anaerobic condition at 55°C. The enrichment culture was sequentially sub-cultured into a series of 5–10 serum bottles (dilution 10^{-6}- 10^{-11}), introducing 10% inoculum into each of them. From the last serum bottle, in which the growth and formation of bio-H_2(g) were recorded, re-inoculation was repeated on a series of serum bottles.

Incubation of Thermoanaerobacterium thermosaccharolyticum SP-H2 was carried out at 55°C in the dark on a thermostat shaker with 100 rpm.

2.1.2 Conducting Batch Test for Microorganisms

Batch experiments were carried out in 60 ml serum bottles with a working volume of ≈20 ml containing 2 ml (10% v/v) of the strain SP-H2 suspension at exponential phase (OD600=0.8-1.0), 18 ml of Pfennig`s medium, [72]. Cheese whey was added as the carbon source. The volume of cheese whey added was 5.0 ml, respectively. The chemical oxygen demand (COD) of the added substrate in all bottles was 3840 mg O_2/l. The initial pH of the medium was adjusted to 7.0 with a 10% solution of HCl or NaOH. The serum bottles were closed with rubber stoppers and aluminum caps and purged with nitrogen gas to create anaerobic conditions. During the dark fermentation, biogas components and soluble metabolite products (SMPs) were monitored. Control serum bottles did not contain any carbon source, except endogenous carbon from cell suspension and some components (yeast extract, cysteine) of the medium. The hydrogen production in the control bottles were subtracted from the hydrogen production in treatment bottles to obtain the actual hydrogen production from wastewater by

SP-H2. Incubation was carried out at 55°C in the dark on a thermostat shaker with 100 rpm. All treatments were conducted in triplicates.

2.2 Experimental Set-up

The experiments were conducted by an up-flow anaerobic continuous plug flow reactor (ACPFR) packed with immobilization materials. ACPFR is a tube reactor. The tube reactor diameter was 10 cm, whereas the length of the reactor was 45 cm to achieve a total working volume of 3.53 liter. The outer shell, which is a cylinder with a central rotation axis, was also considered. A packed bed reactor should have 4 times more length than diameter to achieve the best-packed biofilm composition. The volume of the reactor was 3532.5 cm^3 (3.53 l). The packed bed reactor density was 0.94 g/cm^3, and its porosity was 85%. The geometry was divided into a number of discrete cells, and the governing equations were solved numerically until the time-step horizon was converged for a transient study.

The DEM coupled with CFD was used to create a packed bed with a spherical particle tube reactor. Bio-H_2(g) production on the immobilized culture was via a continuously operated biofilm as a 2.1 mm thickness layer on the packed bed. The inlet was a liquid, while gaseous effluent was collected at the top side of the reactor. A mesh refinement study was made during grid spacing by reducing the factor from 0.5 to 0.0025 mm until the results were unremarkably changed with the grid size reduction. It was found that 0.015 mm is fine enough to obtain grid-independent results. The total number of mesh elements was 0.15984 ml. Overall, the mesh provided the best accuracy and was adopted for the CFD simulation. To estimate the grid convergence uncertainty of the CFD solution, this study used the grid convergence index (GCI) method based on the Richardson extrapolation. The initial wall boundary y + spacing remained the same for each grid refinement level.

2.3 Analytical Methods

The biogas composition was analyzed by a gas chromatography–mass spectrometry (GC-MS); a gas chromatograph (GC) (Agilent Technology model 6890N) equipped with a mass selective detector (Agilent 5973 inert MSD) by injecting a sample volume of 2 ml. Mass spectra were recorded using a VGTS 250 spectrometer equipped with a capillary SE 52 column (HP5-MS 30 m, 0.25 mm ID, 0.25 μm) at 220°C with an isothermal program for 10 min. The initial oven temperature was kept at 50°C for 1 min, then raised to 220°C at 25°C/min and from 200 to 300°C at 8°C/min, and was then maintained for 5.5 min. High purity Helium [He(g)] was used as the carrier gas at constant flow mode (1.5 ml/min, 45 cm/s linear velocity). The calibration was carried out with a standard gas composed of 25% CO_2(g), 2% O_2(g), 10% N_2(g) and 63% CH_4(g), respectively.

Bio-H_2(g) was measured with GC-MS (Agilent 6890N GC - Agilent 5973 inert MSD) according to the above operating parameters. In addition to VFAs (acetic, butyric, and propionic acids) were analyzed at the end of the experimental set-up. After centrifugation (13000 rpm, 30 min), VFA concentrations were measured by same GC-MS (Agilent Technology model 6890N GC - Agilent 5973 inert MSD). The gas carrier of the flow was nitrogen [N_2(g)].

All experimental parameters were measured according to the Standard Methods (2022), [28].

2.4 Kinetics Model for Bio-H_2(g) Production

The reaction kinetic model was created using the Andrews substrate inhibition model with *Thermotoga neapolitana* microorganisms, [75]. *Thermotoga neapolitana* is a rod-shaped, gram-negative bacterium, [76], distinguishable by a thick periplasmic cell wall, [77]. They are generally 0.2-5 μm in size, but can also reach sizes up to 100 μm. It is sporeless, with its rod shape and gram-negative features, and is characteristic of the order *Thermotogales*, [77]. *Thermotoga neapolitana* is considered thermophilic, with a habitable temperature range of 50–95°C. The optimum temperature is 77°C, making it almost hyperthermophilic, [77]. There is also evidence that it can be found in saline environments due to its ability to grow in moderately halophilic environments, [78].

The kinetic model of bio-H_2(g) production was used *Thermotoga neapolitana* bacteria with the Andrews model of substrate inhibition in Eq. (1), [75]:

$$q_L^{H_2} = q_{L,max}^{H_2} \, x \, \frac{S}{K_s + S + \frac{S^2}{K_L}} \quad (1)$$

where;$q_{L,max}^{H_2}$: is the maximum H_2(g) specific production rate (mmol H_2/g.h), S: is the substrate concentration (g/l) and K_s: is the inhibition constant (g/l), respectively.

2.4.1 Computational Fluid Dynamic (CFD) Model

The kinetics conservation equation was implemented in the CFD software by UDF function written in C code. The model contains protein, which makes up ≈ 27-30% of the dry weight of *Thermotoga neapolitana* bacteria. A numerical CFD study of hydrodynamics-biokinetics aspects for interactions between multiphase is an important part of how hydrodynamics influence biokinetics for bio-H_2(g) production. This numerical model contains kinetics information, which is applicable to a set of process parameters, thereby complicating process analysis and the design of the fermentation system. Adoption of kinetics models is also complicated across different studies making application of process analysis and design of fermentation system.

CFD modeling involves the use of numerical methods and algorithms to solve the fundamental governing equations of fluid dynamics (i.e. continuity, momentum, and energy equations). In traditional CFD software, the solutions to these equations are found by solving a set of partial differential equations called the Navier-Stokes equations. The Navier-Stokes equations describe the motion of a fluid and how the pressure, velocity, temperature, and density of a moving fluid are related. For a three-dimensional (3D) system, they consist of one continuity equation for the conservation of mass, three equations for the conservation of momentum, and one equation for the conservation of energy, [79].

The continuity equation is presented in Eq. (2), and it states that the mass in the control volume cannot be created, destroyed, or transformed:

$$\frac{D_\rho}{D_t} + \rho \nabla . V = 0 \qquad (2)$$

where, ρ: is the density, t: is the time, and (∇.V): is the divergence of the velocity vector field, respectively.

Traditional CFD packages are used to solve partial differential equations related to fluid flow; It uses finite volume, finite difference, or finite element methods. The use of advanced methods for simulating fluid flows, such as the mesh Boltzmann method, [80], and the computational fluid dynamics/discrete element method, [81], or meshless methods, such as smoothed particle hydrodynamics, [82], has increased over the last few years.

The use of CFD to study and optimize slurry anaerobic digesters has already been undertaken by several authors, [83], [84], [85]. In general, the hydrodynamics of common sludge anaerobic digesters can be adequately simulated assuming single-phase (liquid) or two-phase (gas/liquid) flow, as shown in most studies reviewed, [86]. A common approach to model the rheological behaviour of slurry digesters is to use a non-Newtonian model for the liquid phase. This allows the model to account for the effects of the total solids content in the viscosity of the wastewater without having to include a solid phase in the model, hence reducing the number of phases to be simulated, [84], [87], [88]. In general, this is a reasonably good assumption as the size of the solids dispersed on the flow is very small compared to the size of the reactors.

For high-rate anaerobic granular sludge reactors (AGSRs), such as up-flow anaerobic sludge blanket (UASB) reactors, expanded granular sludge bed (EGSB) reactors, and internal circulation (IC) reactors; The role of biogas bubbles, the influence of the granules and the influence of the mixture should not be underestimated. UASB reactors are thought to be self-mixing by the upstream movement of biogas bubbles and liquid flow through the reactor, [89]. Additionally, high-rate systems can retain biomass granules (high solids residence time). This is ensured by a combination of reactor design, settling characteristics of the granules, and liquid up-flow velocity. An accurate CFD model would include the effects of biogas bubbles on the overall flow characteristics. It would also capture the effects of increased flow rates of wastewater and biogas on the loss of biomass (sludge wash-out). In this context, CFD simulations stand out as a tool capable of aiding in the design and study of AGSRs by allowing for design iterations for optimizations without the need to construct and build reactors.

The use of CFD for the simulation of AGSRs has begun in the last two decades; however, multiphase simulations are generally computationally demanding, especially when a granular (solid) phase is included. Furthermore, a CFD model should only be used to guide real-life design decisions if it has been carefully verified and validated, [90]. Therefore, knowing the state of the art in terms of previous studies and validated models will enable the development of further research.

Previously, published studies in the field focused on CFD applied to anaerobic digesters in a more general approach, without focusing on granular reactors, [26], [27], [86], [91]. Other reviews focused on aspects such as protocols for the simulations and validation of the models, [24], [92]. The use of CFD applied to specific tasks such as

modeling of mixing in anaerobic digestion reactors has been the core of some reviews, [93], [94], [95].

Modeling of anaerobic granular reactors has been studied from the perspective of hydrodynamics and general modeling, [96], [97]. Modeling of granular sludge reactors (aerobic, anaerobic, and nitriding-anammox) is reviewed from a mechanistic modeling perspective (i.e., mass balance-based models with transport and reaction terms), [25]. Some studies have reported using CFD to study the transport of solid, liquid and gas phases, [25]. While we discuss the forces involved in momentum transfer between phases, no details are given about CFD modeling.

2.4.2 Artificial Neural Network (ANN) Model

An ANN model coming from the simulation results for the considered gasification system, relying on features and output matrixes, is established. The research aim is to develop an ANN model linked with an equilibrium for the estimation of the specific mass flow rate of H_2(g) production (sm_{H2}) from different operating conditions (HRTs, pH, and feed rate). Then, an attempt is made to investigate the relative impact of biomass properties and operating parameters on sm_{H2}. At the end, to have a comprehensive analysis, variations of the inputs on sm_{H2} regarding H_2(g) content are compared and analyzed together.

The ANNs always consist of three layers including (i) input, (ii) hidden, and (iii) output layers. The outputs of a neuron are calculated using Eq. (3):

$$o = f\left(\sum_{j=0}^{n} \omega_j \, x \, X_j\right) \tag{3}$$

where, n: is the input number, x_j: is the j^{th} input to the neutron, ω_j: is the j^{th} synaptic weight, and f: is a non-linear function, respectively.

For converting output data between – 1 and + 1, the hyperbolic tangent formula was applied as Eq. (4):

$$\tanh(x) = \frac{2}{1+ e^{-2x}} - 1 \tag{4}$$

During the training process of input and output data set, the network weights are adjusted to achieve the similar outputs as seen in the training data set. For this purpose, the data were divided into two subsets for training model and validation purposes.

The Pearson correlation coefficient (r^2) and mean standard error (MSE) were computed to evaluate the performance of the developed models according to the following formulas, [98], as Eq. (5) and Eq. (6):

$$r^2 = 1 - \frac{\sum_{i=1}^{N}\left(y_{pre,i} - y_{exp,i}\right)^2}{\sum_{i=1}^{N}\left(y_{pre,i} - y_{ave}\right)^2} \tag{5}$$

$$MSE = \frac{1}{N}\sum_{i=1}^{N}\left(\left|y_{pre,i} - y_{exp,i}\right|\right)^2 \tag{6}$$

In order to avoid numerical overflows related to very large or small weights, all of data were converted to normalized values using as Eq. (7):

$$x_{norm} = 0.8\, x\, \left(\frac{x_i - x_{min}}{x_{max} - x_{min}}\right) + 0.1 \tag{7}$$

Due to lack of related studies, the performance and efficiency of ACPFR for biological H_2(g) production and wastewater treatment in different experimental conditions for bio-H_2(g) production were evaluated in the present study. In addition, the ANN model was developed to predict the performance of the ACPFR for wastewater treatment and bio-H_2(g) production.

ANN predicts the output of a process given the values of process input and process control variables, [99]. It is often used to model relationships between large sets of varying data. ANN can either feed the results to an operator to make process control adjustments or implement appropriate control adjustments automatically, [99]. Many researchers have used this type of approach with great success and recommended the use of neural network models especially when the exact relationship between inputs and outputs is not known and where strong non-linear relationships exist. It was reported that the real-life anaerobic process for biogas yield is very complex, [100], and non-linear, [101], as well as highly dependent on different substrate characteristics, [102], and various operating conditions such as organic loading rate, pH, retention time, carbon/nitrogen ratio, temperature, pressure, agitation rate, etc., [103]. However, one way to understand the relationships between the substrates' characteristics and the optimum biogas yield is through machine learning facilitated by models and equations, [104]. However, determining an exact mathematical model is rigorous because the relationships are very complex and highly non-linear, [99].

2.5 Other Artificial Intelligence Techniques

Artificial intelligence has found a wide range of applications in many fields such as environmental sciences, agricultural sciences, basic and applied sciences, anthropological studies, medical fields, and general engineering family. To achieve reasonable and logical results; They are used to

model, predict, and simulate processes. Modeling a multivariate system; It is quite difficult due to the complexity of processes that exhibit non-linear behavior, which are difficult to describe with linear mathematical models, [104]. Therefore, artificial intelligence technology can predict nonlinear relationships extremely quickly and reliably. Advances in computing power are minimizing the time required to develop models as well as the time required to retrain models to incorporate new data and reflect process changes. The four main types of artificial intelligence approaches based on major branches are summarized and shown in Figure 3 (Appendix), [105]:

Artificial intelligence can be developed without quantifying the micro-scale interactions that occur. In the anaerobic process, such interactions are often poorly understood, thus making it impossible to develop useful mechanistic process models. Instead of this, several researchers have applied artificial intelligence techniques to optimize the dark fermentation process. While it is understood that the application of artificial intelligence in biogas production is still a growing phenomenon, its application in bio-H_2(g) production is still a very new application.

Nature-inspired computing (NIC) is a recently developed branch of artificial intelligence techniques. Natural systems (living and non-living) have an innate ability to evolve, often in parallel and against each other, in a dialectic way. The harmony, beauty, and vigor of life underlie this complexity of evolution. Even without a central control, the processing of information happens in a distributed, self-organized, and optimal way. Equilibrium is maintained in nature through optimal searching, and this forms the basis of algorithm development for optimization problems in process engineering.

Algorithms are iterative procedures for providing calculations or guidelines in a step-wise manner tailored for specific goals. Computational optimization aims to create algorithms to design, implement, and test for solving optimization problems, [106].

Optimization works on various levels, including maximization of performance, efficiency, and profit, or minimization of energy and economics. If infinite time were available, any problem could be solved, but that is not the case with real situations. When time and resources are constrained, intelligent techniques are required. To address non-linear systems like the dark fermentation process in an ACPFR, computer simulation becomes an indispensable tool.

3 Results and Discussions

3.1 CFD Model for Bio-H_2(g) Production from ACPFR

Three-dimensional, unstable, incompressible, multiphase CFD tube reactor model to simulate bio-H_2(g) production from ACPFR; The Lagrangian-Eulerian approximation was implemented with a two-stage model using the appropriate Reynolds stress closure solved by boundary conditions. The fluid flow was laminar according to the general criteria of Reynolds number (Re) at the inlet. The fluid properties were constant except for the formulation of the buoyancy term. The governing equations of continuity are Eq. (8) and momentum Eq. (9) can be written as follows:

$$\frac{\partial \rho}{\partial t} + \nabla . (\rho \vec{v}) = 0 \quad (8)$$

$$\frac{\partial}{\partial t}(\rho \vec{v}) + \nabla . (\rho \vec{v} \vec{v}) = -\nabla p + \nabla \vec{\sigma} + \rho \vec{g} + \vec{F} \quad (9)$$

where, ρ: is the volume average density, $\vec{v}$: is the flow velocity, p: is the static pressure, $\vec{\sigma}$: is the stress tensor, $\rho\vec{g}$ represents the gravitational body force and $\vec{F}$ represents the external force.

The continuity equation for the gas phase is shown as Eq. (10):

$$\frac{\partial \varepsilon_g \rho_g}{\partial t} + \nabla . \left(\varepsilon_g \rho_g \overrightarrow{v_g}\right) - R_g \quad (10)$$

where, ρ_g: is the gas density, $\overrightarrow{v_g}$: is the gas velocity, R_g: is the interphase mass transfer terms for the gas-solid interface reactions, and ε_g: is the volume fraction of the gas phase.

The energy equation for a fluid region is given by Eq. (11):

$$\frac{\partial}{\partial t}(ph) + \nabla . (\rho h \vec{v}) = \nabla . [(k + k_l) \nabla T] + S_h \quad (11)$$

where, ρ, k, T and S_h: are the density, molecular conductivity, temperature and the volumetric heat source, respectively; $\vec{v}$: is the flow velocity, while k_l: is the heat conductivity due to turbulent transport.

The momentum equation for the gas phase is Eq. (12):

$$\frac{\partial \varepsilon_g \rho_g \overrightarrow{v_g}}{\partial t} + \nabla . \left(\varepsilon_g \rho_g \overrightarrow{v_g}\, \overrightarrow{v_g}\right) - \nabla . \overrightarrow{S_g} + \sum_{m=1}^{M} \vec{l}\, \vec{g}\, s_m + \varepsilon_g \rho_g \vec{g} \quad (12)$$

where, $\overrightarrow{S_g}$: is the second order stress tensor of the gas, $\vec{I}$: is the interaction force representing momentum transfer between the gas and solid phase, $\vec{g}$: is the gravitational force, and s_m: is the mass source.

The gas species is Eq. (13):

$$\frac{\partial \rho_g Y_i}{\partial t} + \nabla.\left(\rho_g Y_i \overrightarrow{v_g}\right) - \nabla.\left(\rho_g D_{eff} \nabla Y_i\right) + S_{pi_{Yi}} + S_{Y_i} \quad (13)$$

where, D_{eff}: is the effective mass diffusion coefficient, Y_i: is the mass fraction of gas species, I, $S_{pi_{Yi}}$: is the species source term from the particle, and S_{Y_i}: is the species source term from reactions, respectively.

The liquid phase of continuity and momentum equations are Eq. (14) and Eq. (15):

$$\frac{\partial}{\partial t}(\alpha_l \rho_l) + \nabla.(\alpha_l \rho_l v_l) = 0 \quad (14)$$

$$\frac{\partial}{\partial t}(\alpha_l \rho_l v_l) + \nabla.(\alpha_l \rho_l v_l v_l) = -\alpha_l \nabla \rho_l - \nabla.(\alpha_l T^v + \alpha_l T^R) + \alpha_l \rho_l g + S_M \quad (15)$$

where, α_l: is the void fraction of the fluid phase, ρ_l: is the density of the fluid phase, v_l: is the velocity of the fluid phase, T^v: is the momentum viscous tensor, T^R: is the Reynolds tensor and S_M: is the momentum of the source term.

3.2 Simulations of Numerical

The Lagrangian–Eulerian approach is adopted to describe the biomass slurry flow behavior of the liquid–gas phase in laminar flow. Both phases were treated as a continuous process that intertwined and interacted with each other in the computational domain. The recirculation flow rate coefficient was 0.32. Initial and boundary conditions are shown in Table 1. The operating temperature was between 30 and 45°C. This long-term simulation lasted 40 days. The concentration of gaseous products (H_2, CH_4, etc.) and soluble metabolites such as VFAs (acetic acids, butyric acids, and propionic acids) were evaluated at specified time intervals throughout all operational phases.

All terms of the governing equations are discrete using the second-order upwind scheme. The PRESTO (pressure staggering option) algorithm was used for the pressure-velocity coupling. The Green-Gauss cell-based method was used for the discretization of the gradient. Each case was simulated in ANSYS Fluent 2016 software (Cannonsburg, PA, USA) with the initialization procedure for simulations with second-order schemes. Convergence was evaluated based on the low mass flow rate imbalance below 1.0×10^5 kg/s. The second step was to generate an ANSYS Fluent (Cannonsburg, PA, USA) journal file to automatically run the flow case with the prescribed boundary conditions from the algorithm for the pressure, flow rate, and temperature. The numerical simulations were performed on an i7-3770 CPU 3.70 GHz processer Intel computer with 16 GB RAM and a 64-bit operating system.

3.3 The Effect of Increasing HRTs for Bio-H_2(g) Production at ACPFR

Increasing HRTs values (1, 2, 4, 8, and 12 days) were examined in MSW with Thermoanaerobacterium thermosaccharolyticum SP-H2 methane bacteria during dark fermentation for bio-H_2(g) production in ACPFR, at 37°C (Fig. 4). 0.070, 0.109, 0.121 and 0.078 mg/l.h bio-H_2(g) production rates were measured for 1, 2, 4, and 12 days HRTs, respectively, in ACPFR after dark fermentation process, at 37°C (Figure 4, Appendix). The maximum 0.134 mg/l.h bio-H_2(g) production rate was observed for 8 days HRTs in ACPFR after dark fermentation process at 37°C (Figure 4, Appendix).

The bio-H_2(g) yield in different fractions of ACPFR was 0.201-0.567 mg/h/l. ACPFR reactor temperature was 25°C and HRT was 2 hours. Bio-H_2(g) concentrations filled the packed bed differently. The fluid velocity profile is laminar, with maximum velocity occurring at the center of the ACPFR. It was observed that the temperature gradient occurred only at the ACPFR inlet due to heat transfer from the ACPFR wall.

0.952, 1.067, 1.183 and 1.075 mol H_2/mol substrate bio-H_2(g) yields were obtained for 1, 2, 4 and 12 days HRTs, respectively, in ACPFR after dark fermentation process, at 37°C (Fig. 5). The maximum 0.202 mol H_2/mol substrate Bio-H_2(g) yield was found for 8 days HRTs in ACPFR after dark fermentation process, at 37°C (Figure 5, Appendix).

3.4 The Effect of Different pH Values for Bio-H_2(g) Production at ACPFR

Different pH values (4.0, 5.0, 6.0, 7.0 and 8.0) were examined in MSW with Thermoanaerobacterium thermosaccharolyticum SP-H2 methane bacteria during dark fermentation for bio-H_2(g) production in ACPFR, at 37°C (Fig. 6). 0.94, 1.03, 0.85 and 0.69 kmol/m^3 bio-H_2(g) production values were measured for pH=4.0, pH=5.0, pH=7.0, pH=8.0

respectively, in ACPFR after dark fermentation process, at 37°C (Figure 6, Appendix). The maximum 1.22 kmol/m^3 bio-H_2(g) production value was found for pH=6.0 in ACPFR after dark fermentation process at 37°C (Figure 6, Appendix).

The model of dark fermentation shows that the most optimal pH for the bio-H_2(g) production process is ≈ pH=5.0-6.0. Lowering pH effectively reduces the process of methanogenesis, simultaneously increasing bio-H_2(g) production.

3.5 The Effect of Increasing Feed Rate as OLR for Bio-H_2(g) Production at ACPFR

Increasing feed rates as OLR values (0.5, 1, 2, 4, 8, and 10 g COD/l.d) were operated in MSW with Thermoanaerobacterium thermosaccharolyticum SP-H2 methane bacteria during dark fermentation for bio-H_2(g) production in ACPFR, at 37°C (Figure 7, Appendix). 1.36, 1.22, 1.14, 0.81 mol H_2/mol substrate bio-H_2(g) yields were observed for 1, 2, 4, 8 and 10 g COD/l.d OLR, respectively, in ACPFR after dark fermentation process, at 37°C (Figure 7, Appendix). The maximum 1.61 mol H_2/mol substrate bio-H_2(g) yield was obtained for 0.5 g COD/l.d OLR in ACPFR after dark fermentation process at 37°C (Figure 7, Appendix).

The increase of OLR up to 8 g COD/l.d has a negative effect on the biological H_2(g) yield. This situation may be due to VFAs accumulation at higher OLR, in addition, the supersaturation of H_2(g) in liquid phase may be related to the lower biogas production and relieving inhibition due to bio-H_2(g) production, [107].

3.6 The Measurements of VFAs after Bio-H_2(g) Production at ACPFR

Different VFAs (acetic acid, butyric acid, and propionic acid) were observed in MSW with Thermoanaerobacterium thermosaccharolyticum SP-H2 methane bacteria during dark fermentation in ACPFR, at 37°C (Figure 8, Appendix). 52%, 55%, 58%, and 61% acetic acid proportions were measured for 1, 2, 4, and 8 days HRTs, respectively, in ACPFR after dark fermentation, at 37°C (Figure 8, Appendix). 73% maximum acetic acid value was found for 12 days HRTs in ACPFR after dark fermentation process, at 37°C (Figure 8, Appendix).

18%, 22%, 19%, and 4% butyric acid proportions were observed for 2, 4, 8, and 12 days HRTs, respectively, in ACPFR after dark fermentation process, at 37°C (Fig. 8). 25% maximum butyric acid value was obtained for 1 day HRTs in ACPFR after dark fermentation process, at 37°C (Figure 8, Appendix).

23%, 20%, 20%, and 22% propionic acid proportions were measured for 1, 4, 8, and 12 days HRTs in ACPFR after dark fermentation process, at 37°C (Figure 8, Appendix). The maximum 27% propionic acid value was observed for 2 days HRTs in ACPFR after dark fermentation process, at 37°C (Figure 8, Appendix).

3.7 The Comparison between Experimental Bio-H_2(g) Production Yield and ANN Values in ACPFR

A comparison between experimental values of bio-H_2(g) production yields and the predicted ANN values (Figure 9, Appendix). The value of R^2 for the ANN model was found to be up to 0.98 (data not shown). 0.952, 1.067, 1.183, 1.202, and 1.075 mol H_2/mol substrate bio-H_2(g) production yields were measured for 1, 2, 4, 8, and 12 days HRTs, respectively, in ACPFR after dark fermentation process, at 37°C (Figure 9, Appendix).

0.947, 1.056, 1.175, 1.199 and 1.071 mol H_2/mol substrate ANN values were observed for 1, 2, 4, 8, and 12 days HRTs, respectively, from ANN simulation (Figure 9, Appendix). The ANN was an excellent model because of the lowest error and the highest coefficient values. The obtained results indicated that the simulation model based on the ANN is practical.

4 Conclusions

The maximum is 0.134 mg/l.h bio-H_2(g) production rate was observed for 8 days HRTs in ACPFR after dark fermentation process at 37°C.

The maximum 0.202 mol H_2/mol substrate Bio-H_2(g) yield was found for 8 days HRTs in ACPFR after dark fermentation process, at 37°C

The maximum 1.22 kmol/m^3 bio-H_2(g) production value was found for pH=6.0 in ACPFR after dark fermentation process at 37°C. The model of dark fermentation shows that the most optimal pH for the bio-H_2(g) production process is ≈ pH=5.0-6.0. Lowering pH effectively reduces the process of methanogenesis, simultaneously increasing bio-H_2(g) production.

The maximum 1.61 mol H_2/mol substrate bio-H_2(g) yield was obtained for 0.5 g COD/l.d OLR in ACPFR after the dark fermentation process at 37°C.

73% maximum acetic acid value was found for 12 days HRTs in ACPFR after dark fermentation process, at 37°C.

25% maximum butyric acid value was obtained for 1 day HRTs in ACPFR after dark fermentation process, at 37°C.

The maximum 27% propionic acid value was observed for 2 days HRTs in ACPFR after dark fermentation process, at 37°C.

Reduced H_2(g) content is caused by the production of CO_2(g) by bacteria species that do not produce bio-H_2(g). Moreover, short HRT increases the rate of substrate conversion and generates higher substrate flow. For HRT equal to 1 h, acetic acid dominates because the productivity of metabolites decreases with decreasing HRT with decreasing substrate conversion. The acetic pathway is the most effective pathway in the dark fermentation process. The acetic fermentative pathway was the main route for bio-H_2(g) production. The fermentative pathway implied hydrogen in reduced metabolites. The low biomass retention may contribute to the changing metabolic pathways of acetogenic bacteria.

The use of validated CFD models to predict the multiphase flow, accounting for the interfacial momentum transfer between the three phases present in ACPFR is still a challenge. It is generally accepted that the ultimate goal of having validated multiphase CFD models is the coupling with biokinetics models for accurate modeling of the biogas generation within the reactors, once hydrodynamics and biochemical effects are interdependent in ACPFR. A functional coupled CFD-biokinetics model would allow for the scale-up of processes while correctly predicting the generation of biogas, and also taking into consideration realistic mixing conditions within the ACPFR. Some of the main challenges and hence opportunities for future work towards this end goal are listed hereafter.

The first and more complex challenge is the inclusion to predict biomass degradation as well as biogas generation. For that to be possible, a three-phase CFD model must be used to account for the biomass as well as the biogas inside the ACPFR.

The granules' apparent density is not fixed, as it is linked to the biogas generated. Including the effects of the granular apparent density changes due to bubble entrapment/attachment would lead to a better prediction of the movement of the granules in the sludge bed as well as the effects of granular wash-out. Therefore, leading to a more accurate prediction of loss of biomass.

The established ANN-based model in this work indicates satisfactory and sound results with an R^2 value of more than 0.980 and an RMSE value lower than 0.25 for $sm_{hydrogen}$ as a product from a gasification system connected with a H_2(g) plant. Almost all of the inputs show a significant impact on the $sm_{hydrogen}$ output. Significantly, gasifier temperature, SBR, moisture content, and H_2(g) have the highest impacts on the $sm_{hydrogen}$ with contributions of 19.85%, 17.29%, 15.41%, and 11.53%, respectively. In addition, other variables of feed properties like carbon (C), oxygen (O), sulphur (S) and nitrogen (N) contribute in the range of 1.31%–9.4% and proximate components like VM, FC and A contribute in the range of 3.21%–7.71% to the impact on $sm_{hydrogen}$.

It also examined the adaptability, governing equations, processing time, flexibility, and applicability of artificial intelligence in dark fermentation process in an ACPFR for bio-H_2(g) production. In addition to, this study established that artificial intelligence modeling has the potential to drastically reduce the process development time for dark fermentation process in an ACPFR at anaerobic conditions of substrates, although at varying degrees.

The accurate results obtained for bio-H_2(g) production through the gasification system connected to ACPFR reactors confirm the strong predictive ability of the developed ANN-based model by applying a backpropagation algorithm with a hidden layer of 13 neurons. The developed model has the ability to be used with a wide range of biomass. The results show the relative influence of various biomass properties and operating parameters on the bio-H_2(g) output from the system. Finally, the developed ANN model can be practically used to screen suitable biomasses for H_2(g) extraction based on a gasification system connected to W-G shifting and H_2(g) recovery unit.

Developing standardized and practical procedures for selecting algorithm and determining dataset size. Developing such procedures will require a comprehensive understandings of the impacts/effectiveness of different algorithms and training data samples to solve various bioenergy problems. More case studies for bioenergy systems with different biomass feedstock, conversion technologies, and products will be needed.

CFD has proven useful in evaluating reactor performance; It allows local and instantaneous analysis of reaction rate; interphase hydrogen flows and other processes taking place within the tank. Numerical simulations were used to study bio-H_2(g) production and removal at different times to evaluate the local behavior of the equipment and suggest geometric changes. Experimental results show that bio-H_2(g) production significantly reduces production costs; It clearly shows the opportunity to be used as an environmentally friendly biofuel.

Process design, modeling, and simulation of bio-H_2(g) production in an ACPFR; It represents an essential tool for process optimization and scale-up. Bio-H_2(g) process efficiency production depends significantly on the type of substrate from various sources. Furthermore, in the process of scaling up experimental parts to real application and commercialization; Different bioreactor configurations combined with kinetic models will be realized.

Acknowledgement:
This research study was undertaken in the Environmental Microbiology Laboratories at Dokuz Eylül University Engineering Faculty Environmental Engineering Department, İzmir, Turkey. The authors would like to thank this body for providing financial support.

References:

[1] G.Peixoto, N.K. Saavedra, M.B.A. Varesche, M. Zaiat, Hydrogen production from soft-drink wastewater in an upflow anaerobic packed-bed reactor, *International Journal of Hydrogen Energy*, Vol.36, 2011, pp. 8953–8966.

[2] A.D.N. Ferraz Junior, C. Etchebehere, M. Zaiat, High organic loading rate on thermophilic hydrogen production and metagenomic study at an anaerobic packed-bed reactor treating a residual liquid stream of a Brazilian biorefinery, *Bioresource Technology*, Vol.186, 2015, pp. 81–88.

[3] M.Y. Azwar, M.A. Hussain, A.K. Abdul-Wahab, Development of biohydrogen production by photobiological, fermentation and electrochemical processes: A review, *Renewable and Sustainable Energy Reviews*, Vol.31, 2014, pp. 158–173.

[4] A. Smolinski, K. Stanczyk, N. Howaniec, Steam gasification of selected energy crops in a fixed bed reactor, *Renewable Energy*, Vol.35, 2010, pp. 397–404.

[5] N. Howaniec, A. Smolinski, Biowaste utilization in the process of co-gasification with bituminous coal and lignite, *Energy*, Vol.118, 2017, pp. 18–23.

[6] G. Kumar, S. Shobana, D. Nagarajan, D.J. Lee, K.S. Lee, C.Y. Lin, C.Y. Chen, J.S. Chang, Biomass based hydrogen production by dark fermentation: Recent trends and opportunities for greener processes, *Current Opinion in Biotechnology*, Vol.50, 2018, pp. 136–145.

[7] B. Lumbers, D.W. Agar, J. Gebel, F. Platte, Mathematical modeling and simulation of the thermo-catalytic decomposition of methane for economically improved hydrogen production, *International Journal of Hydrogen Energy*, Vol.47, 2022, pp. 4265–4283.

[8] M.R. Talaghat, N. Naamaki, Mathematical modeling of hydrogen production using methanol steam reforming in the coupled membrane reactor when the output materials of the reformer section are used as feed for the combustion section, *International Journal of Hydrogen Energy*, Vol.46, 2021, pp. 2282–2295.

[9] K. Christopher, R. Dimitrios, A review on exergy comparison of hydrogen production methods from renewable energy sources, *Energy and Environmental Sciences*, Vol.5, No.5, 2012, pp. 6640-6651.

[10] M.M. Amin, B. Bina, E. Taheri, M.R. Zare, M. Ghasemian, S.W. Van Ginkel, A. Fatehizadeh, Metabolism and kinetic study of bioH2 production by anaerobic sludge under different acid pretreatments, Process Biochemistry, Vol.61, 2017, pp. 24-29.

[11] T. Lipman, *An Overview of Hydrogen Production and Storage Systems with Renewable Hydrogen Case Studies*, Montpelier: Clean Energy States Alliance; 2011.

[12] P.C. Hallenbeck, D. Ghosh, Advances in fermentative biohydrogen production: the way forward? *Trends in Biotechnology*, Vol.27, No.5, 2009, pp. 287-297.

[13] L.B. Brentner, J. Peccia, J.B. Zimmerman, Challenges in developing biohydrogen as a sustainable energy source: implications for a research agenda, *Environmental Science & Technology*, Vol.44, No.7, 2010, pp. 2243-54.

[14] P. Sivagurunathan, G. Kumar, P. Bakonyi, S.H. Kim, T. Kobayashi, K.Q. Xu, G. Lakner, G. Toth, N. Nemestothy, K. Belafi-Bako, A critical review on issues and overcoming strategies for the enhancement of dark fermentative hydrogen production in continuous systems, *International Journal of Hydrogen Energy*, Vol.41, 2016, 3820e36.

[15] Y. Wong, T. Wu, J. Juan, A review of sustainable hydrogen production using seed sludge via dark fermentation, *Renewable*

and Sustainable Energy Reviews, Vol.34, 2014, pp. 471-482.

[16] M. Agler, B. Wrenn, S. Zinder, L. Angenent, Waste to bioproduct conversion with undefined mixed cultures: the carboxylate platform, *Trends in Biotechnology*, Vol.29, 2011, pp. 70-78.

[17] Y. Chen, Y. Yin, J. Wang, Recent advance in inhibition of dark fermentative hydrogen production, *International Journal of Hydrogen Energy,* Vol.46, 2021, pp. 5053-5073.

[18] M. Aydin, A. Karaca, A.M. Qureshy, I. Dincer, A comparative review on clean hydrogen production from wastewaters, *Journal of Environmental Management*, Vol.279, 2021, 111793.

[19] M.P. Sudhakar, B.R. Kumar, T. Mathimani, K. Arunkumar, A review on bioenergy and bioactive compounds from microalgae and macroalgae-sustainable energy perspective, *Journal of Cleaner Production*, Vol.228, 2019, pp. 1320–1333.

[20] H. Zhu, W. Parker, R. Basnar, A. Proracki, P. Falletta, M. Béland, P. Seto, Buffer requirements for enhanced hydrogen production in acidogenic digestion of food wastes, *Bioresource Technology*, Vol.100, 2009, pp. 5097–5102.

[21] C.L. Alvarez-Guzmán, S. Cisneros-de la Cueva, V.E. Balderas-Hernández, A. Smolinski, A. De Leon-Rodriguez, Biohydrogen production from cheese whey powder by Enterobacter asburiae: Effect of operating conditions on hydrogen yield and chemometric study of the fermentative metabolites, *Energy Reports*, Vol.6, 2020, pp. 1170–1180.

[22] Z. Trad, J.P. Fontaine, C. Larroche, C. Vial, Multiscale mixing analysis and modeling of bio-hydrogen production by dark fermentation, *Renewable Energy*, Vol.98, 2016, pp. 264–282.

[23] X. Wang, J. Ding, W.Q. Guo, N.Q. Ren, A hydrodynamics reaction kinetics coupled model for evaluating bioreactors derived from CFD simulation, *Bioresource Technology*, Vol.101, 2010, pp. 9749–9757.

[24] I. Nopens, D. Sudrawska, W. Audenaert, D. Fernandes del Pozo, U. Rehman, Water and wastewater CFD and validation: are we losing the balance? *Water Science and Technology*, Vol.81, 2020, pp. 1636–1645.

[25] J.E. Baeten, D.J. Batstone, O.J. Schraa, M.C.M. van Loosdrecht, E.I.P. Volcke, Modelling anaerobic, aerobic and partial nitritation-anammox granular sludge reactors - A review, *Water Research*, Vol.149, 2019, pp. 322–341.

[26] R.W. Samstag, J.J. Ducoste, A. Griborio, I. Nopens, D.J. Batstone, J.D. Wicks, S. Saunders, E.A. Wicklein, G. Kenny, J. Laurent, CFD for wastewater treatment: an overview, *Water Science and Technology,* Vol.74, 2016, pp. 549–563.

[27] B. Wu, Advances in the use of CFD to characterize, design and optimize bioenergy systems, *Computers and Electronics in Agriculture*, Vol. 2013, pp. 195–208.

[28] W.C. Lipps, E.B. Braun-Howland, T.E. Baxter, *Standard Methods for the Examination of Water and Wastewater*, (24th. Edition), W.C. Lipps, E.B. Braun-Howland, T.E. Baxter, (editors), American Public Health Association (APHA), American Water Works Association (AWWA), Water Environment Federation (WEF), Elevate Your Standards. American Public Health Association 800 I Street, NW Washington DC: 20001-3770, USA, December 1, 2022; ISBN:9780875532998.

[29] J.S. Chang, K.S. Lee, P.J. Lin, Bio-hydrogen production with fixed-bed bioreactors, *International Journal of Hydrogen Energy,* Vol.27, 2002, pp. 1167–1174.

[30] G. Kumar, A. Mudhoo, P. Sivagurunathan, D. Nagarajan, A. Ghimire, C.H. Lay, C.Y. Lin, D.J. Lee, J.S. Chang, Recent insights into the cell immobilization technology applied for dark fermentative hydrogen production, *Bioresource Technology*, Vol.219, 2016, pp. 725–737.

[31] G. Kumar, G. Buitrón, Fermentative bio-hydrogen production in fixed bed reactors using ceramic and polyethylene carriers as supporting material, *Energy Procedia*, Vol.142, 2017, pp. 743–748.

[32] F. Hawkes, I. Hussy, G. Kyazze, R. Dinsdale, D. Hawkes, Continuous dark fermentative hydrogen production by mesophilic microflora: Principles and progress. Int. J. Hydrogen Energy 2007, 32, 172–184.

[33] Saady, N.M.C. Homoacetogenesis during hydrogen production by mixed cultures dark fermentation: Unresolved challenge, *International Journal of Hydrogen Energy*, Vol.38, 2013, pp. 13172–13191.

[34] A. Wodołazski, Co-simulation of CFD-multiphase population balance coupled model aeration of sludge flocs in stirrer tank bioreactor, *International Journal of Multiphase Flow*, Vol.123, 2020, pp. 103–162.

[35] T. Weide, E. Brugging, C. Wetter, A. Ierardi, M. Wichern, Use of organic waste for biohydrogen production and volatile fatty acids via dark fermentation and further processing to methane, *International Journal of Hydrogen Energy*, Vol.44, 2019, pp. 24110–24125.

[36] R.Y. Kannah, S. Kavitha, P. Sivashanmugham, G. Kumar, D.D. Nguyen, S.W. Chang, J.R. Banu, Biohydrogen production from rice straw: Effect of combinative pretreatment, modeling assessment and energy balance consideration, *International Journal of Hydrogen Energy*, Vol.44, 2019, pp. 2203–2215.

[37] P.C. Ri, J.S. Kim, T.R. Kim, C.H. Pang, H.G. Mun, G.C. Pak, N.Q. Ren, Effect of hydraulic retention time on the hydrogen production in a horizontal and vertical continuous stirred-tank reactor, *International Journal of Hydrogen Energy*, Vol.44, 2019, pp. 17742–17749.

[38] H. Chen, A.S. Kim, Prediction of permeate flux decline in crossflow membrane filtration of colloidal suspension: a radial basis function neural network approach, *Desalination*, Vol.192, No.1-3, 2006, pp. 415-428.

[39] W.-Q. Guo, N.-Q. Ren, Z.-B. Chen, B.-F. Liu, X.-J. Wang, W.-S. Xiang, J. Ding, Simultaneous biohydrogen production and starch wastewater treatment in an acidogenic expanded granular sludge bed reactor by mixed culture for long-term operation, *International Journal of Hydrogen Energy*, Vol.33, No.24, 2008, pp. 7397-7404.

[40] M. Sadrzadeh, T. Mohammadi, J. Ivakpour, N. Kasiri, Neural network modeling of Pb^{2+} removal from wastewater using electrodialysis, *Chemical Engineering and Processing-Process Intensification*, Vol.48, No.8, 2009, pp. 1371-1381.

[41] A.K. Giri, R.K. Patel, S.S. Mahapatra, Artificial neural network (ANN) approach for modeling of arsenic (III) biosorption from aqueous solution by living cells of Bacillus cereus biomass, *Chemical Engineering Journal*, Vol.178, 2011, pp. 15-25.

[42] L. Chen, S. Nguang, X. Li, X. Chen, Soft sensors for on-line biomass measurements, *Bioprocess and Biosystems Engineering*, Vol.26, 2004, pp. 191-195.

[43] P. Poirazi, F. Leroy, M.D. Georgalaki, A. Aktypis, L. De Vuyst, E. Tsakalidou, Use of artificial neural networks and a gamma-concept-based approach to model growth of and bacteriocin production by Streptococcus macedonicus ACA-DC 198 under simulated conditions of kasseri cheese production, *Applied and Environmental Microbiology*, Vol.73, 2007, pp. 768-776.

[44] P. Escalante-Minakata, V. Ibarra-Junquera, H. Rosu, A. De León-Rodríguez, R. González García, On-line monitoring of Mezcal fermentation based on redox potential measurements, *Bioprocess and Biosystems Engineering*, Vol.32, 2009, pp. 47-52.

[45] S. Frigo, G. Spazzafumo, Cogeneration of power and substitute of natural gas using biomass and electrolytic hydrogen, *International Journal of Hydrogen Energy*, Vol.43, 2018, pp. 11696–11705.

[46] Q. Li, G. Song, J. Xiao, T. Sun, K. Yang, Exergy analysis of biomass staged-gasification for hydrogen-rich syngas, *International Journal of Hydrogen Energy*, Vol.44, 2019, pp. 2569–2579.

[47] N. Kobayashi, M. Tanaka, G. Piao, J. Kobayashi, S. Hatano, Y. Itaya, S. Mori, High temperature air-blown woody biomass gasification model for the estimation of an entrained down-flow gasifier, *Journal of Waste Management*, Vol.29, 2009, pp. 245–251.

[48] T. Damartzis, S. Michailos, A. Zabaniotou, Energetic assessment of a combined heat and power integrated biomass gasification–internal combustion engine system by using aspen plus®, *Fuel Processing Technology*, Vol.95, 2012, pp. 37–44.

[49] T.L.T. Nguyen, J.E. Hermansen, R.G. Nielsen, Environmental assessment of gasification technology for biomass conversion to energy in comparison with other alternatives: The case of wheat straw, *Journal of Cleaner Production*, Vol.53, 2013, pp. 138–148.

[50] A. Porcu, S. Sollai, D. Marotto, M. Mureddu, F. Ferrara, A. Pettinau, Techno-economic analysis of a small-scale biomass-

to energy bfb gasification-based system, *Energies*, Vol.12, 2019, 494.

[51] D. Roy, S. Samanta, S. Ghosh, Thermo-economic assessment of biomass gasification-based power generation system consists of solid oxide fuel cell, supercritical carbon dioxide cycle and indirectly heated air turbine, *Clean Technologies and Environmental Policy*, Vol.21, 2019, pp. 827–845.

[52] S. Safarian, C. Richter, R. Unnthorsson, Waste biomass gasification simulation using aspen plus: Performance evaluation of wood chips, sawdust and mixed paper wastes, *International Journal of Power and Energy Engineering*, Vol.7, 2019, pp. 12–30.

[53] S. Safarian, R. Unnþórsson, C. Richter, A review of biomass gasification modeling, *Renewable and Sustainable Energy Reviews*, Vol.110, 2019, pp. 378–391.

[54] S. Safarian, R. Unnthorsson, C. Richter, Techno-economic analysis of power production by using waste biomass gasification, *International Journal of Power and Energy Engineering*, Vol.8, 2020, pp. 1–8.

[55] S. Safarian, R. Unnthorsson, C. Richter, Performance analysis and environmental assessment of small-scale waste biomass gasification integrated chp in Iceland, *Fermentation*, Vol.197, 2020, 117268.

[56] S. Safarian, R. Unnthorsson, C. Richter, Simulation of small-scale waste biomass gasification integrated power production: A comparative performance analysis for timber and wood waste, *International Journal of Applied Power Engineering (IJAPE)*, Vol.9, 2020, pp. 147–152.

[57] S. Safarian, R. Unnthorsson, C. Richter, Techno-economic and environmental assessment of power supply chain by using waste biomass gasification in Iceland, *Biophysical Economics and Sustainability*, Vol.5, No.7, 2020, pp. 1-13.

[58] J. Gil, J. Corella, M.A.P. Aznar, M.A. Caballero, Biomass gasification in atmospheric and bubbling fluidized bed: Effect of the type of gasifying agent on the product distribution, *Biomass and Bioenergy*, Vol.17, 1999, pp. 389–403.

[59] E. Shayan, V. Zare, I. Mirzaee, Hydrogen production from biomass gasification; a theoretical comparison of using different gasification agents, *Energy Conversion and Management*, Vol.159, 2018, pp. 30–41.

[60] V. Marcantonio, M. De Falco, M. Capocelli, E. Bocci, A. Colantoni, M. Villarini, Process analysis of hydrogen production from biomass gasification in fluidized bed reactor with different separation systems, *International Journal of Hydrogen Energy*, Vol.44, 2019, pp. 10350–10360.

[61] V. Rostampour, A.M. Motlagh, M.H. Komarizadeh, M. Sadeghi, I. Bernousi, T. Ghanbari, Using artificial neural network (ann) technique for prediction of apple bruise damage, *Australian Journal of Crop Science*, Vol.7, 2013, pp. 1442–1448.

[62] J. George, P. Arun, C. Muraleedharan, Assessment of producer gas composition in air gasification of biomass using artificial neural network model, *International Journal of Hydrogen Energy*, Vol.43, 2018, pp. 9558–9568.

[63] V. Nasir, S. Nourian, S. Avramidis, J. Cool, Classification of thermally treated wood using machine learning techniques, *Wood Science and Technology*, Vol.53, 2019, pp. 275–288.

[64] V. Nasir, S. Nourian, S. Avramidis, J. Cool, Prediction of physical and mechanical properties of thermally modified wood based on color change evaluated by means of "group method of data handling" (gmdh) neural network, *Holzforschung*, Vol.73, 2019, pp. 381–392.

[65] G. Capizzi, G.L. Sciuto, C. Napoli, M. Wozniak, G. Susi, A spiking neural network-based long-term prediction system for biogas production, *Neural Networks*, Vol.129, 2020, pp. 271–279.

[66] S. Safarian, S.M.E. Saryazdi, R. Unnthorsson, C. Richter, Artificial neural network integrated with thermodynamic equilibrium modeling of downdraft biomass gasification-power production plant, *Energy*, Vol.213, 2020, 118800.

[67] M. Puig-Arnavat, J.A. Hernández, J.C. Bruno, A. Coronas, Artificial neural network models for biomass gasification in fluidized bed gasifiers, *Biomass and Bioenergy*, Vol.49, 2013, pp. 279–289.

[68] D. Baruah, D. Baruah, M. Hazarika, Artificial neural network-based modelling of biomass gasification in fixed bed downdraft gasifiers, *Biomass and Bioenergy*, Vol.98, 2017, pp. 264–271.

[69] A. Schmidt, W. Creason, B.E. Law, Estimating regional effects of climate change and altered land use on biosphere

carbon fluxes using distributed time delay neural networks with bayesian regularized learning, *Neural Networks*, Vol.108, 2018, pp. 97–113.

[70] S. Safarian, S.M.E. Saryazdi, R. Unnthorsson, C. Richter, Artificial neural network modeling of bioethanol production via syngas fermentation, *Biophysical Economics and Sustainability*, Vol.6, 2021, pp. 1–13.

[71] A.A. Kovalev, D.A. Kovalev, Y.V. Litti, I.V. Katraeva, Biohydrogen production in the two-stage process of anaerobic bioconversion of organic matter of liquid organic waste with recirculation of digester effluent, *International Journal of Hydrogen Energy*, Vol.45, No.51, 2020, pp. 26831–26839.

[72] N. Pfennig, Anreicherungskulturen fürote und grüne Schwefelbakterien, *Zentralblatt Fur Bakteriologie Mikrobiologie Und Hygiene I- Abteilung Originale C-Allgemeine Angewandte Und Okologische Mikrobiologie*, Vol.1, 1965, pp. 179–189.

[73] N. Pfenning, K.D. Lippert, Über das Vitamin B12 Bedürfnis phototropher Schwefelbakterien, *Archives of Microbiology*, Vol.55, 1966, pp. 245–246.

[74] E.A. Wolin, M.J. Wolin, R.S. Wolfe, Formation of methane by bacterial extracts, *Journal of Biological Chemistry*, Vol.238, 1963, pp. 2882–2886.

[75] D. Frascari, M. Cappelletti, J.D.S. Mendes, A. Alberini, F. Scimonelli, C. Manfreda, L. Longanesi, D. Zannoni, D. Pinelli, S. Fedi, A kinetic study of bio-hydrogen production from glucose, molasses and cheese whey by suspended and attached cells of Thermotoga neapolitana, *Bioresource Technology*, Vol.147, 2013, pp. 553–561.

[76] S.A. Van Ooteghem, S.K. Beer, P.C. Yue, Hydrogen production by the thermophilic bacterium Thermotoga Neapolitana, *Applied Biochemistry and Biotechnology*, Vol.98–100, No.1–9, 2002, pp. 177–189.

[77] S. Belkin, C.O. Wirsen, H.W. Jannasch, A new sulfur-reducing, extremely Thermophilic Eubacterium from a submarine thermal vent, *Applied and Environmental Microbiology*, Vol.51, No.6, 1986, pp. 1180–1185.

[78] E. Windberger, R. Huber, A. Trincone, H. Fricke, K.O. Stetter, Thermotoga Thermarum Sp. Nov. and Thermotoga Neapolitana occurring in African continental solfataric springs, *Archives of Microbiology*, Vol.151, No.6, 1989, pp. 506–512.

[79] J. Anderson, *Computational Fluid Dynamics: The Basics with Applications*, 1st ed. In: J.P. Holman, J.R. Lloyd, (Eds.). McGraw-Hill Education, New York, NY, USA, 1995.

[80] Z.G. Feng, E.E. Michaelides, E.E., The immersed boundary-lattice Boltzmann method for solving fluid–particles interaction problems, *Journal of Computational Physics*, Vol.195, No.2, 2004, pp. 602–628.

[81] H.R. Norouzi, R. Zarghami, N. Mostoufi, New hybrid CPU-GPU solver for CFD-DEM simulation of fluidized beds, *Powder Technology*, Vol.316, 2017, pp. 233–244.

[82] M. Meister, W. Rauch, Wastewater treatment modeling with smoothed particle hydrodynamics, *Environmental Modelling, and Software*, Vol.75, 2016, pp. 206–211.

[83] B. Wu, E.L. Bibeau, Development of 3-D anaerobic digester heat transfer model for cold weather applications, *Transactions of the ASABE*, Vol.49, 2006, pp. 749–757.

[84] B. Wu, S. Chen, CFD simulation of non-Newtonian fluid flow in anaerobic digesters, *Biotechnology and Bioengineering*, Vol.99, 2008, pp. 700–711.

[85] S. Dabiri, P. Kumar, C. Ebner, W. Rauch, On the effect of biogas bubbles in anaerobic digester mixing, *Biochemical Engineering Journal*, Vol.173, 2021, 108088.

[86] C. Sadino-Riquelme, R.E. Hayes, D. Jeison, A. Donoso-Bravo, Computational fluid dynamic (CFD) modelling in anaerobic digestion: general application and recent advances, *Critical Reviews in Environmental Science and Technology*, Vol.48, 2018, pp. 39–76.

[87] P.A. Lopez-Jimenez, J. Escudero-Gonzalez, T. Montoya Martínez, V. Fajardo Montanana, C. Gualtieri, Application of CFD methods to an anaerobic digester: the case of Ontinyent WWTP, Valencia, Spain, *Journal of Water Process Engineering*, Vol.7, 2015, pp. 131–140.

[88] S. Shrestha, S.P. Lohani, CFD analysis for mixing performance of different types of household biodigesters, *Clean Energy*, Vol.6, 2022, pp. 325–334.

[89] C.A. de Lemos Chernicharo, 2007. *Anaerobic Reactors*, Biological Treatment Wastewater Series, Vol.4, IWA Publishing,

London, United Kingdom, 2007, ISBN 1: 1-84339 164 3, ISBN 13: 9781843391647.

[90] S. Safarianbana, R. Unnthorsson, C. Richter, Development of a New Stoichiometric Equilibrium-Based Model for Wood Chips and Mixed Paper Wastes Gasification by Aspen Plus, In ASME International Mechanical Engineering Congress and Exposition; American Society of Mechanical Engineers: Salt Lake City, UT, USA, 2019, V006T006A00.

[91] D.J. Batstone, D. Puyol, X. Flores-Alsina, J. Rodríguez, Mathematical modelling of anaerobic digestion processes: applications and future needs, *Reviews in Environmental Science and Biotechnology*, Vol.14, 2015, pp. 595–613.

[92] J. Laurent, R.W. Samstag, J.M. Ducoste, A. Griborio, I. Nopens, D.J. Batstone, J.D. Wicks, S. Saunders, O. Potier, A protocol for the use of computational fluid dynamics as a supportive tool for wastewater treatment plant modelling, *Water Science and Technology*, Vol.70, 2014, pp. 1575–1584.

[93] J. Lindmark, E. Thorin, R. Bel Fdhila, E. Dahlquist, Effects of mixing on the result of anaerobic digestion: review, *Renewable and Sustainable Energy Reviews*, Vol.40, 2014, pp. 1030–1047.

[94] G. Leonzio, Studies of mixing systems in anaerobic digesters using CFD and the future applications of nanotechnologies, *Waste and Biomass Valorization*, Vol.11, 2020, pp. 5925–5955.

[95] J. Li, M. Suvarna, L. Li, L. Pan, J. Perez-Ramírez, Y.S. Ok, X. Wang, A review of computational modeling techniques for wet waste valorization: research trends and future perspectives, *Journal of Cleaner Production*, Vol.367, 2022, 133025.

[96] F. Liotta, P. Chatellier, G. Esposito, M. Fabbricino, E.D. van Hullebusch, P.N.L. Lens, F. Pirozzi, Current views on hydrodynamic models of nonideal flow anaerobic reactors, *Critical Reviews in Environmental Science and Technology*, Vol.45, 2015, pp. 2175–2207.

[97] J. Yang, *Approaches for Modelling Anaerobic Granule-Based Reactors*, Bacterial Biofilms, S. Dincer, M. Sümengen Özdenefe, A. Arkut (Eds.), IntechOpen, London, United Kingdom, 2020, number of pages: 360. https://doi.org/10.5772/intechopen.90201, ISBN: 978-1-78985-900-3.

[98] U. Özdemir, B. Özbay, S. Veli, S. Zor, Modeling adsorption of sodium dodecyl benzene sulfonate (SDBS) onto polyaniline (PANI) by using multi linear regression and artificial neural networks, *Chemical Engineering Journal*, Vol.178, 2011, pp. 183-190.

[99] V.V. Nair, H. Dhar, S. Kumar, A.K. Thalla, S. Mukherjee, J.W.C. Wong, Artificial neural network-based modeling to evaluate methane yield from biogas in a laboratory-scale anaerobic bioreactor, *Bioresource Technology*, Vol.217, 2016, pp. 90–99.

[100] W. Uddin, K. Ayeshab, Z. Kamran, H. Aun, K. Bilal, I. Saiful, M. Ishfaqa, K. Imran, M. Adild, K. Hee Je. 2019. Current and future prospects of small hydropower in Pakistan: A survey, *Energy Strategy Reviews*, Vol.24, 2019, pp. 166–177.

[101] C. Rashama, G. Ijoma, T. Matambo, Biogas generation from by-products of edible oil processing: a review of opportunities, challenges and strategies, *Biomass Conversion and Biorefinery Journal*, Vol.9, No.4, 2019, pp. 803–826.

[102] K.C. Surendra, D. Takara, A.G. Hashimoto, S.K. Khanal. 2014. Biogas as a sustainable energy source for developing countries, *Opportunities and Challenges Renewable and Sustainable Energy Reviews*, Vol.31, 2014, pp. 846–859.

[103] R. Arthur, M.F. Baidoo, E. Antwi. Biogas as a potential renewable energy source: A Ghanaian case study, *Renewable Energy*, 13, 2010, pp. 1–7

[104] M.M. Ghiasi, M. Arabloo, A.H. Mohammadi, T. Barghi, Application of ANFIS soft computing technique in modeling the CO_2 capture with MEA, DEA, and TEA aqueous solutions, *International Journal of Greenhouse and Gas Control*, Vol.49, 2016, pp. 47–54.

[105] S.A. Kalogirou, Artificial intelligence for the modeling and control of combustion processes: A review, *Progress in Energy and Combustion Science*, Vol.29, No.6, 2003, pp. 515–566.

[106] F. Manzano-agugliaro, F.G. Montoya, C. Gil, A. Alcayde, J. Gómez, R. Banose, Optimization methods applied to renewable and sustainable energy: A review, *Renewable and Sustainable Energy Reviews*, Vol.15, 2011, pp. 1753–1766.

[107] S.W. Van Ginkel, B. Logan, Increased biological hydrogen production with reduced organic loading, *Water Research*, Vol.39, No.16, 2005, pp. 3819-3826.

APPENDIX

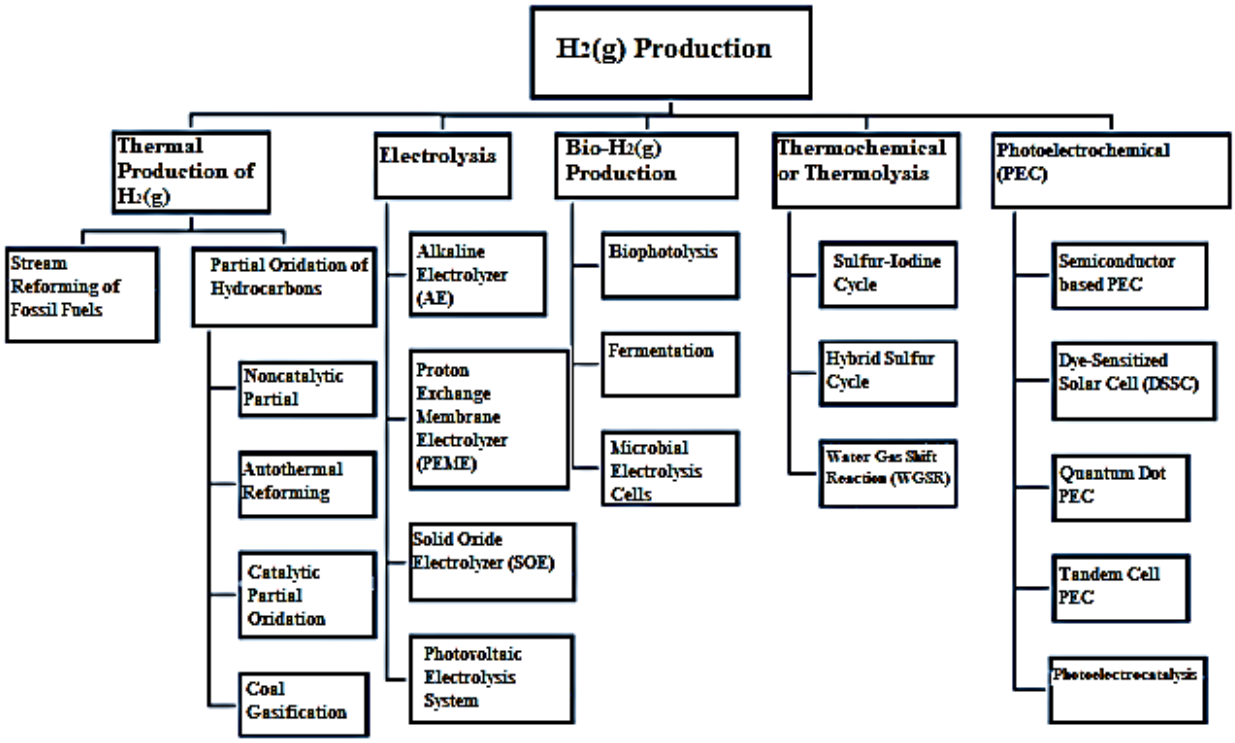

Fig. 1: Different ways of H_2(g) production methods

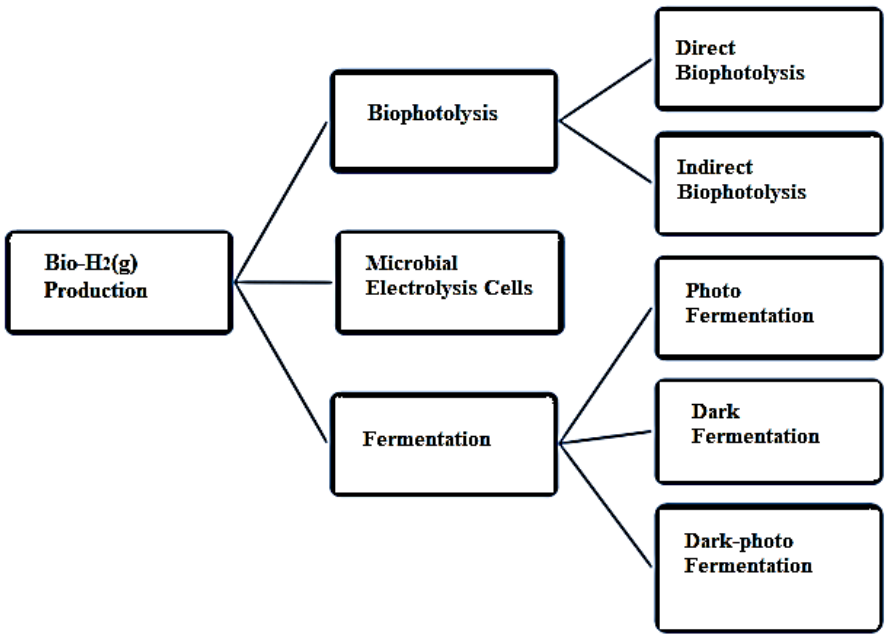

Fig. 2: The methods of bio-H_2(g) production.

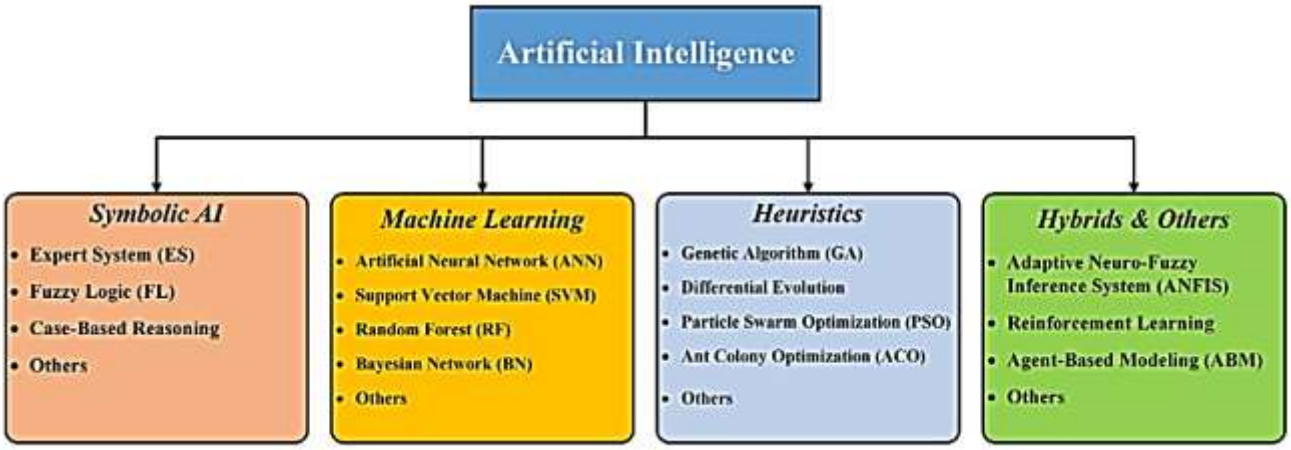

Fig. 3: Artificial intelligence categories and major techniques adopted from, [105].

Table 1. The parameters of initial and boundary conditions

Parameters	**Values**
Inlet flow rate (l/h)	0.2 - 1.0
HRTs (h)	1 - 12
Biomass / substrate ratio	0.154 – 0.352
Temperature (°C)	75 - 250
The size of the solid biomass particles (m)	0.00224 – 0.01167

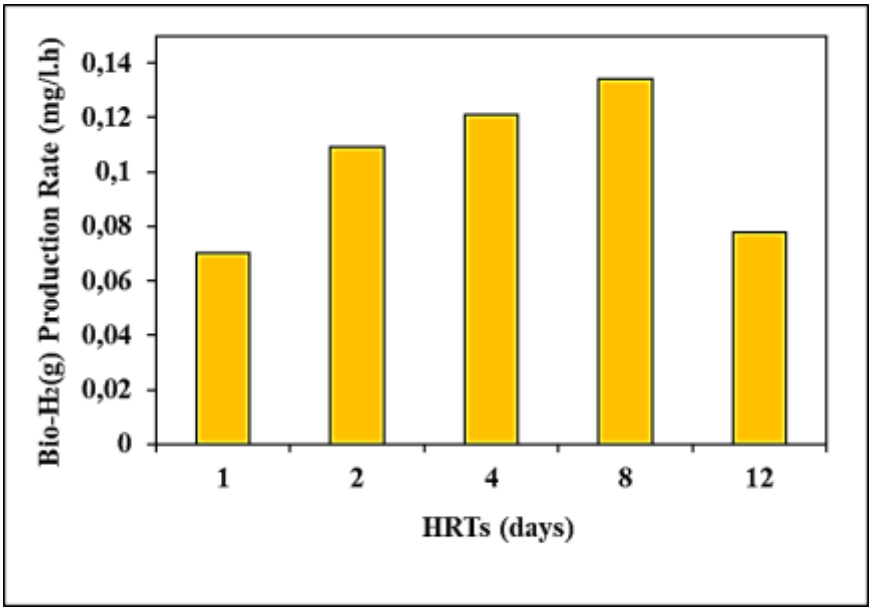

Fig. 4: The effect of increasing HRTs for bio-H_2(g) production rate at ACPFR, at 37°C.

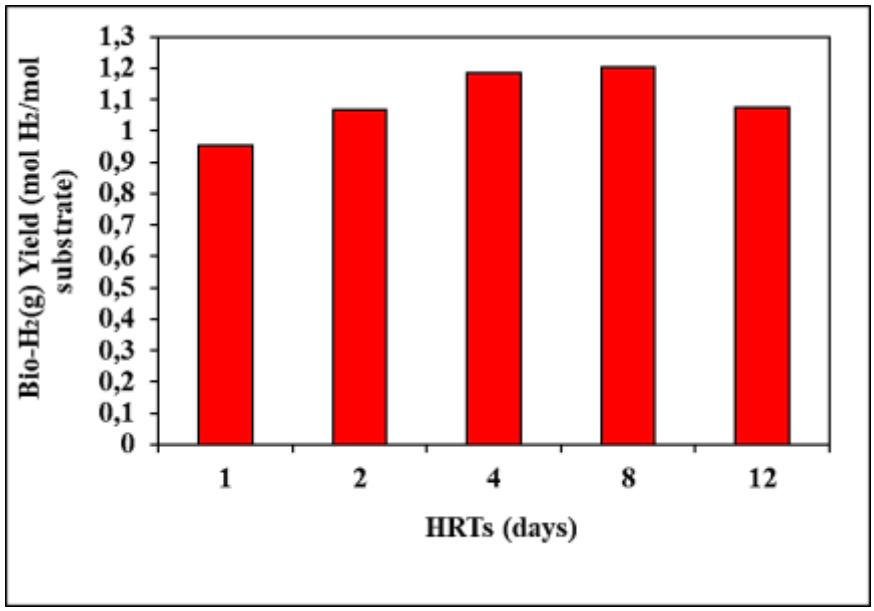

Fig. 5: The effect of increasing HRTs for Bio-H_2(g) production yields at ACPFR, at 37^{o}C.

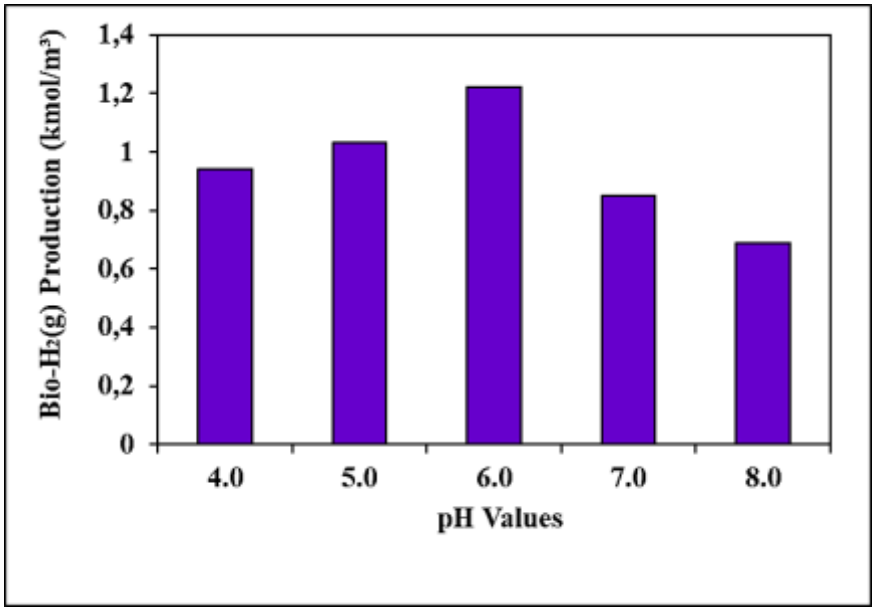

Fig. 6: The Effect of different pH values for bio-H_2(g) production at ACPFR, at 37^{o}C.

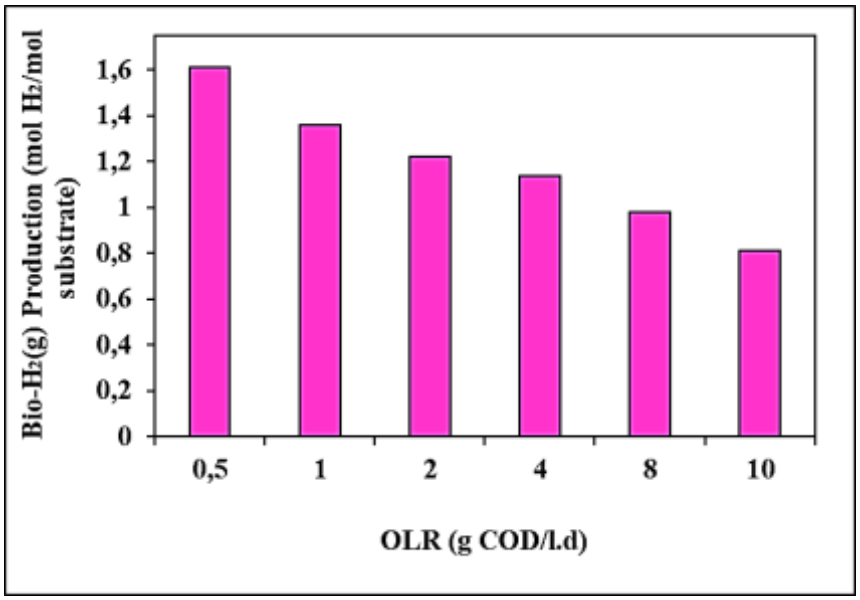

Fig. 7: The effect of increasing feed rate as OLR for bio-H_2(g) production at ACPFR, at 37°C.

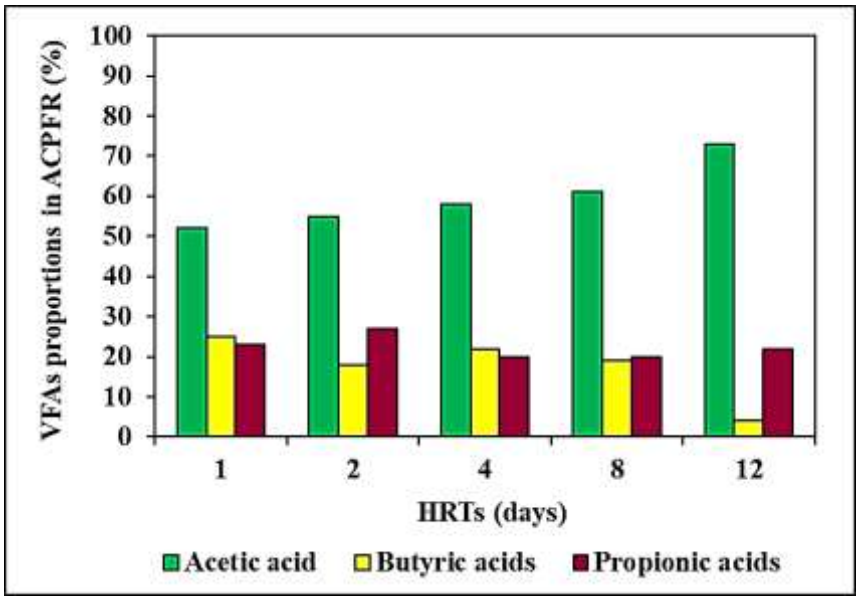

Fig. 8: The measurements of VFAs after bio-H_2(g) production at ACPFR, at 37°C.

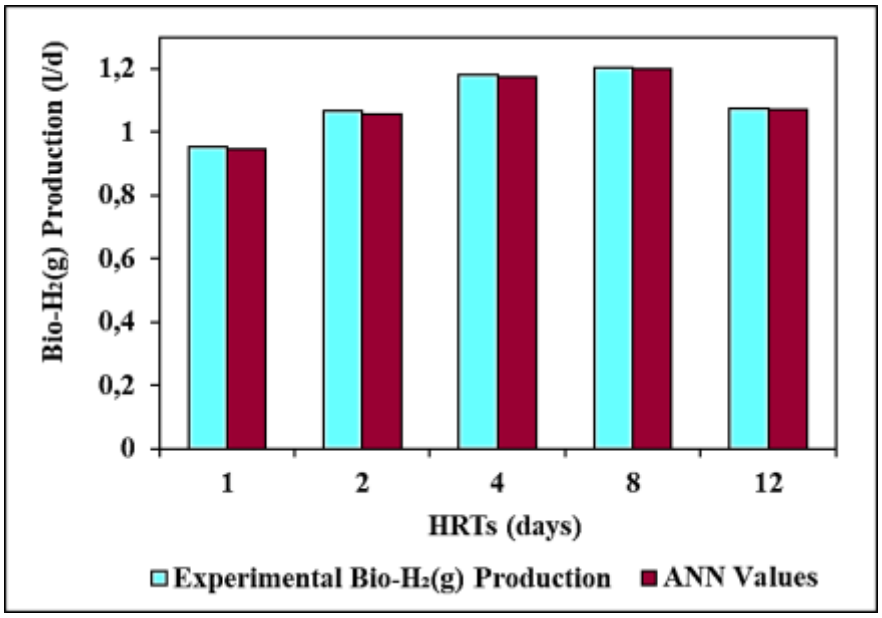

Fig. 9: The comparison between experimental bio-H_2(g) production yields and ANN values in ACPFR, at 37°C.

Contribution of Individual Authors to the Creation of a Scientific Article (Ghostwriting Policy)

Prof. Dr. Delia Teresa Sponza and Post-Dr. Rukiye Öztekin took an active role in every stage of the preparation of this article.

The authors equally contributed in the present research, at all stages from the formulation of the problem to the final findings and solution.

Sources of Funding for Research Presented in a Scientific Article or Scientific Article Itself

This research study was undertaken in the Environmental Microbiology Laboratories at Dokuz Eylül University Engineering Faculty Environmental Engineering Department, İzmir, Turkey. The authors would like to thank this body for providing financial support.

Conflict of Interest

The authors have no conflicts of interest to declare.

Creative Commons Attribution License 4.0 (Attribution 4.0 International, CC BY 4.0)

This article is published under the terms of the Creative Commons Attribution License 4.0
https://creativecommons.org/licenses/by/4.0/deed.en_US